3
Onset of Plasticity in Crystalline Nanomaterials[1)]

Laurent Pizzagalli, Sandrine Brochard, and Julien Godet

1) *This chapter is dedicated to Pierre Beauchamp, who has not only guided the authors into the complex and tortuous world of dislocations for the past 10 years but has also showed them a fair way to behave as a scientist.*

3.1
Introduction

The past two decades have witnessed an amazing development in the fabrication of systems characterized by one or several dimensions in the nanoscale. These so-called nanostructures include, for instance, nanospheres, nanowires, and nanopillars. An intensive research is being done looking for potential applications in various domains such as mechanics, electronics, optoelectronics, photonics, phononics, and so on. The mechanical characterization of these nanomaterials constitutes an important part of this research, since it has been shown that size reduction is often accompanied by large variations in common properties such as strength, hardness, or ductility [1]. For instance, an interesting and intriguing phenomenon is the apparent increase of the ductility range for nanoscale systems compared to the bulk material. Many experiments suggest that nanomaterials could exhibit specific and unusual mechanical properties [2–5], which explains the current interest in the research community and the large number of dedicated studies.

Several limits are commonly used to define the different regimes of the response of a material submitted to a mechanical stress. Among these, the elastic limit, also known as the yield strength, defines the point at which the deformation of the material becomes irreversible, that is, plasticity occurs. Figure 3.1 shows the variation of the yield strength as a function of size for different kinds of nanoscaled systems made of silicon. Obviously, the onset of plasticity is different here compared to bulk materials, with a dramatic increase of strength for smaller sizes. Several mechanisms have been proposed for explaining experimental observations [1].
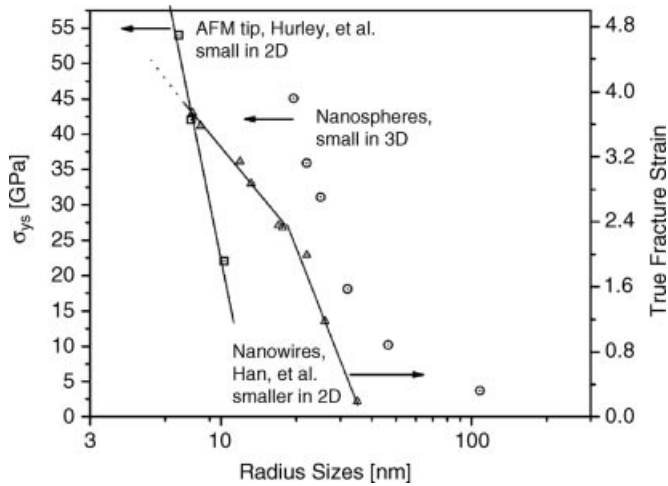
Figure 3.1 Variation of the yield stress (left) and true fracture strain (right) as a function of the size for different nanomaterials. Courtesy of W.W. Gerberich *et al.* [11]

The determination of the yield strength is difficult in general, since it is associated with the onset of plasticity. Usually, the elastic limit and the yield strength correspond to the deviation from linearity in the measured stress–strain curve, although other choices can be made depending on the material. In bulk materials, it depends on the sensitivity of the measurement. In fact, the irreversible displacement of dislocations present in the material may occur even for very low deformation, in the apparent elastic regime. It is therefore difficult to define the onset of plasticity in bulk materials from macroscopic measurements. Its determination is also difficult in the case of nanomaterials, since specific apparatus and techniques are needed for measurements. Additional insights can be obtained from several theoretical approaches, which do not suffer from the same limitations. The issue of the onset of plasticity has been largely examined in the framework of elasticity theory [6–9]. Numerical simulations at the atomistic level also allow reproducing mechanical tests, although they are generally restricted to systems with dimensions closer to tens of nanometers rather than micrometers.

In this chapter, we describe the elastic and atomistic modeling of the onset of plasticity in nanomaterials. Note that we focused on systems including surfaces and for which one or several dimensions are in the nanoscale. This definition not only includes nanopillars and nanowires (1D) and nanospheres (0D) but also supported thin films (2D). Conversely, we did not consider systems characterized by interfaces such as embedded defects (aggregates of point defects, dislocations). Another important issue is the mono- or polycrystalline nature of the nanomaterial. In fact, it has been shown that the plastic properties of nanopillars could strongly depend on their internal structure [10]. For the sake of simplicity, here we focus on monocrystalline materials.

3.2
The Role of Dislocations

The plastic deformation in crystalline materials can be associated with different mechanisms, all involving an irreversible displacement of the matter. The latter can result from the motion of individual atoms (diffusion) or from the collective displacement of atoms in dislocation form. For polycrystalline materials, the plastic deformation can also be due to the rotation and motion of grains. Here, we will consider only the plastic deformation through dislocation nucleation and displacement prior to the failure of the material (fracture). Useful basic information and theory of dislocations in bulk materials can be found in well-known textbooks [8, 9].

In usual bulk materials, the onset of plastic deformation is characterized by the displacement of the dislocations originally present. Depending on the conditions, the later stages of the deformation correspond to the generation of new dislocations, typically through multiplication. Several kinds of mechanisms have been identified [8, 12], the most common one being the Frank–Read and Bardeen–Herring sources, the multiplication by double cross-slip, or the nucleation from surfaces and interfaces. However, it is not clear whether the first mechanisms could be dominant in nanomaterials. In fact, these systems are characterized by one or several dimensions in the nanoscale, which is likely to impede such sources. Furthermore, these mechanisms require the presence of initial defects, usually in very low concentration in nanomaterials. As a consequence, although original multiplication mechanisms specific to nanomaterials have been postulated [13], dislocation nucleation is expected to be the main process in these systems, an assumption supported by experimental observations [14–16] and the obvious fact that the surface/volume ratio is much higher in nanomaterials than in bulk materials. Even in the case where dislocations are present in the system, it has been proposed that these dislocations are first annihilated by escaping to free surfaces, followed by the nucleation of new dislocations [17].

In the following, we focus on the mechanism of dislocation formation from an infinite surface. We first describe the two main forces that will act on a dislocation and the specific case of a dislocation in the vicinity of a surface. The elastic and atomistic modeling of the dislocation nucleation process is then described. Finally, we discuss how these results can be extended to more complex geometries (nanowires) and propose some perspectives.

3.3
Driving Forces for Dislocations

The elastic field associated with dislocations is slowly decaying from the dislocation core according to an inverse power law. Consequently, a dislocation in a real material is expected to interact with many defects (other dislocations, grain boundaries, point defects, surfaces, etc.), all of them exerting a force on the dislocation. However, for our purpose, we first focus on a single isolated dislocation in an otherwise perfect

bulk material. In this case, there are two factors that may change the dislocation configuration in the crystal.

3.3.1
Stress

When a dislocation of Burgers vector **b** with the dislocation line ξ is displaced in the field of a local stress σ, there is a change of energy proportional to the product between the stress and the area swept by the dislocation displacement. Following the definition of a force acting on a dislocation given by Hirth and Lothe [8], it is therefore possible to define a force $\mathbf{F}_\sigma$ acting on an infinitesimal dislocation segment of length l, with the following expression:

$$\frac{\mathbf{F}_\sigma}{l} = (\sigma\mathbf{b}) \times \xi \tag{3.1}$$

which is well known as the Peach–Koehler formula (see Ref. [18] for instance for an explained derivation). This is the driving force for displacing dislocations due to the local stress, and in extenso in a material submitted to a mechanical action.

3.3.2
Thermal Activation

Temperature is the other important factor since it allows overcoming the energy barriers between two different dislocation configurations. Several kinds of thermally activated mechanisms, such as dislocation displacement and unpinning or dislocation core transformations, have been observed or postulated [19]. A usual framework for studying thermally activated mechanisms in materials science is the transition state theory, in particular in its harmonic approximation [20]. Such an approach has been shown to be valid as long as energy barriers are not too small or, equivalently, temperatures are not too high, which is generally the case for dislocations.

It is essential to emphasize that thermal activation does not favor any specific direction, conversely to the mechanical driving force. The displacement of a dislocation under the sole action of temperature is equivalent to a random walk. Also, thermal activation is essentially restricted to spatially localized mechanisms, that is, involving a limited number of atoms. In fact, the probability to perform a specific collective displacement of atoms by thermal motion is rapidly decreasing as a function of the number of atoms.

3.3.3
Combination of Stress and Thermal Activation

Temperature and stress, combined together, will help to overcome the energy barrier associated with a change in the dislocation configuration, leading to a displacement or to a core transformation. The relative importance of each factor depends on the investigated mechanisms. The energy barrier can be overcome, thanks to stress.

For instance, the critical stress required for displacing a dislocation without any thermal activation, that is, at 0 K, is called the Peierls stress. The latter is an important quantity that is usually determined by numerical simulations or by interpolating measurements at finite temperature. Conversely, mechanisms leading to transformation of dislocation cores can be activated only by temperature.

Several regimes can therefore be obtained for a single material, depending on the magnitudes of stress and temperature. Typically, stress is the main driving force in many systems such as metals for an isolated dislocation. But in materials with a high lattice friction such as covalent or geophysical systems, the weight of thermal activation in dislocation-related mechanisms grows. In the case of dislocation nucleation, we will see that both temperature and stress are important.

3.4
Dislocation and Surfaces: Basic Concepts

To study the formation of a dislocation from a surface, it is helpful to first examine the situation where the dislocation is already present in the system and still in interaction with the surface, that is, close enough.

3.4.1
Forces Related to Surface

The presence of a surface introduces an additional complexity in the study of dislocations. In fact, it is well known that there is a long-range interaction on the dislocation due to the surface [9]. This interaction can be understood by considering that the self-energy of a dislocation is decreasing when the dislocation is brought closer to the surface. Alternatively, one can consider that there is relaxation of the stress field of the dislocation by the surface, thus lowering the energy. Another possible subtle effect is the relaxation of the surface stress by the dislocation. The total energy change is equivalent to an attractive force between the dislocation and the surface.

The interaction force between the surface and a dislocation can be derived in the most simple cases using the concept of an image dislocation located in a symmetric position relative to the surface. For a straight edge dislocation with a line parallel to the surface, this force is inversely proportional to the dislocation–surface distance d, and is equal to

$$\frac{F_i}{l} = \frac{Kb^2}{4\pi d} \tag{3.2}$$

where K is a function of the elastic constant parameters depending on the dislocation character. Due to this force, a dislocation segment of length l is drawn closer to the surface. In the specific case of interest here, we consider a half-loop dislocation whose two ends are in connection with the surface (Figure 3.2). This is equivalent to a pinning of the half-loop dislocation by the surface. Therefore, in addition to image interactions, there is an additional line tension force exerted on the half-loop
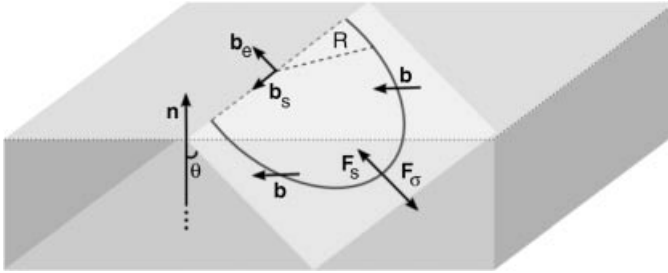
Figure 3.2 Schematic representation of a circular half-loop dislocation of Burgers vector **b** nucleated from a surface and propagating in a slip plane (white), making an angle θ with the surface normal **n**. Edge and screw components of the Burgers vector are $\mathbf{b_e}$ and $\mathbf{b_s}$, relative to the dislocation front. $\mathbf{F_s}$ and $\mathbf{F_\sigma}$ are forces acting on the dislocation associated with surface interaction and stress, respectively.

dislocation that tends to bring the dislocation closer to the surface. In the following, the total force resulting from the interaction of a half-loop dislocation and the surface is called $\mathbf{F_s}$.

3.4.2
Balance of Forces for Nucleation

We now analyze the balance of forces exerted on a spherical half-loop dislocation of radius R, as represented in Figure 3.2. The force $\mathbf{F_s}$ due to the surface tends to bring the dislocation closer to the surface, thereby reducing R. Conversely, for the appropriate stress direction, the force $\mathbf{F_\sigma}$ associated with stress relaxation tends to propagate the dislocation into the material, thus increasing R.

Because these forces are opposed, there is no possible stable configuration. The energy of the half-loop dislocation as a function of R is schematically represented in Figure 3.3. Depending on the value of the stress applied on the dislocation, there are two possible regimes. For low or moderate stress, the energy first increases until it reaches a maximum, defining an unstable equilibrium configuration, and then decreases. This maximum, characterized by an energy E_a and a radius R_c, has to be overcome by thermal activation for nucleating a propagating dislocation. Otherwise, for stress higher than a given value σ_c, the stress contribution is large enough for the energy barrier to vanish, the dislocation formation process becoming athermal. σ_c is the critical stress for nucleating dislocation, comparable to the Peierls stress for displacing dislocation in bulk materials.

3.4.3
Forces Due to Lattice Friction

Up to now, we have discussed the balance of forces for dislocation nucleation from the surface without taking into account the lattice friction of the materials. In fact, to propagate into a material, a dislocation must overcome the lattice resistance, whose
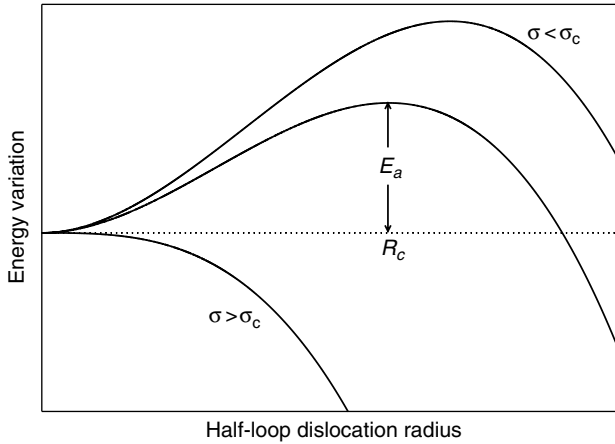
Figure 3.3 Possible energy variations as a function of the radius of a nucleated half-loop dislocation, and definition of the activation parameters for stresses lower than the critical stress σ_c.

magnitude depends on the nature of the material itself. In fcc metallic systems, this resistance is very low and additional barriers in the energy variation can be safely neglected (Figure 3.4). Conversely, in covalent systems, the lattice friction may be very large and these energy barriers could be in the same range or even larger than the activation energy due to surface forces. Then, they have to be considered in the mechanism of dislocation formation from the surface of covalent materials (Figure 3.4). In any case, it is clear that the nucleation of a half-loop dislocation from a surface is possible only if stress and temperature reach values required for dislocation propagation in the bulk.
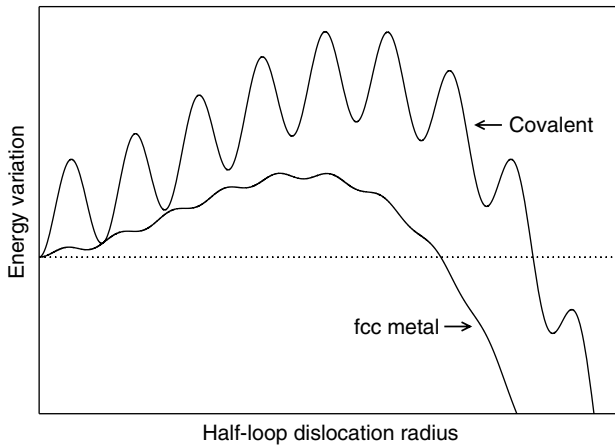

Figure 3.4 Examples of possible energy variations as a function of the radius of a nucleated half-loop dislocation, taking into account the lattice friction for fcc metallic and covalent materials.

3.4.4
Surface Modifications Due to Dislocations

In addition to the above-discussed interaction, a dislocation will change the surface state when it is nucleated or when it leaves the material, which involves an energy variation. The most important (and often visible) surface modification is the creation of a step or a decrease/increase of the height of an existing step. This modification is bounded by the two surface points pinning the half-loop dislocation.

The change of the step height is given by $\pm(\mathbf{b_e} \cdot \mathbf{n})$, $\mathbf{b_e}$ being the edge component of the Burgers vector and $\mathbf{n}$ the surface normal (Figure 3.2). Defining the angle θ between the surface normal $\mathbf{n}$ and the dislocation slip plane, the step height change is $\pm b_e \cos(\theta)$.

3.5
Elastic Modeling

3.5.1
Elastic Model

We aim at determining the energy of the configuration represented in Figure 3.2 in the case of an isotropic medium, relatively to the same system but without the dislocation. In early analyses of dislocation nucleation at surface, it was usually assumed that the self-energy of the half-loop dislocation is simply half the self-energy of a full circular dislocation loop [7–9, 21, 22]. A more accurate formulation has been proposed by Beltz and Freund, who introduced a correction factor m in the logarithmic part of the energy [23]. The self-energy of the circular half-loop is therefore given by

$$U = \frac{\mu b^2 (2-\nu)}{8(1-\nu)} R \left[\ln\left(\frac{8 m \alpha R}{b}\right) - 2 \right] \tag{3.3}$$

In (3.3), μ is the shear modulus, ν is the Poisson coefficient, $\alpha = b/r_0$ is a nondimensional factor defining the unknown dislocation core radius r_0, and m is a geometrical parameter that depends on the Poisson coefficient, the system geometry (angle between surface and slip plane), the shape of the loop, and the Burgers vector orientation. m is necessarily bounded by 0 and 1, but is generally not known. In their seminal work, Beltz and Freund proposed an expression for m in the case of a circular half-loop in a slip plane perpendicular to the surface [23].

The total energy of the system should also include the energy gained by enlarging the dislocation loop, that is, the work associated with stress relaxation. This quantity is proportional to the area swept by the dislocation that is $\pi R^2/2$ in the case of a circular half-loop, yielding

$$W = -\frac{1}{2}\pi R^2 \sigma b \tag{3.4}$$

In the framework of linear isotropic elasticity theory, the latter quantity can also be expressed as a function of the applied deformation ε. In the case of an uniaxial deformation, $\sigma = 2\mu(1+\nu)s\varepsilon$, s being the Schmid factor, and W is now given by

$$W = -\mu b(1+\nu)\pi R^2 s\varepsilon \tag{3.5}$$

A third possible contribution to the total energy is related to surface modifications after dislocation formation. Since the step height change is given by $\pm b_e \cos(\theta)$, the corresponding energy variation is

$$E_s = \pm 2Rb_e \cos(\theta)\gamma_s \tag{3.6}$$

γ_s is equivalent to a surface energy in the case of a high step. When a single step is created in coherence with the crystal structure, $b_e\gamma_s$ is a step energy. Note that very small energy contributions due to dislocation pinning points at the surface are neglected here.

Finally, we have to consider the situations where single partial dislocations are nucleated from the surface. In such case, the propagation of dislocation into the crystal is accompanied with the formation of a stacking fault. Defining the stacking fault energy γ_f, the additional contribution is

$$E_f = \frac{1}{2}\pi R^2 \gamma_f \tag{3.7}$$

Combining (3.3) and (3.4) or (3.5) and (3.6) and eventually (3.7) provides the total energy $E(R, \sigma)$ (or $E(R, \varepsilon)$) associated with the formation of a half-loop dislocation of radius R from a surface for a stress σ (or an applied deformation ε).

It is quite instructive to plot the different contributions to the total energy as a function of R, as shown in Figure 3.5. Here we have selected realistic values for the
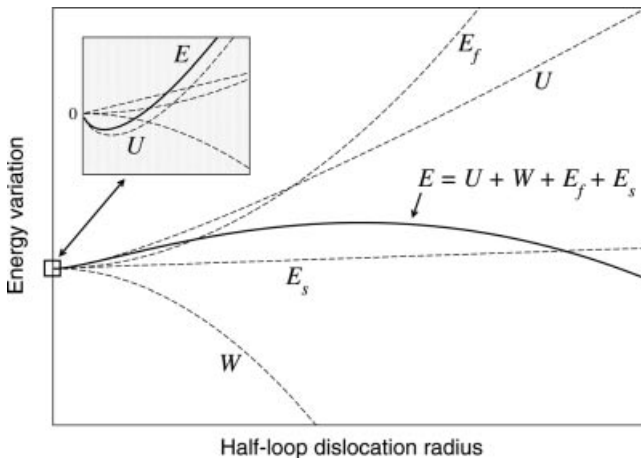

Figure 3.5 Variation of the different energy contributions from the elastic model (described in the text) as a function of the radius of a nucleated half-loop dislocation, using realistic values for the different parameters. Inset shows these variations for a very small radius.

different parameters entering into Eqs (3.3)–(3.7). These correspond to a nucleated partial dislocation with a leading 90° orientation, in aluminum, leaving a step on the surface. For large R, it appears that the step energy E_s is negligible compared to the other contributions. The energy cost E_f for stacking fault creation in the case of partial dislocations, quickly increasing due to the R^2 dependence, is also emphasized. The inset in Figure 3.5 shows the energy variation for small values of R. A local minimum is present in the total energy curve, because of the $R \ln R$ dependence on $U(R)$. This minimum occurs for R values typically lower than the core radius r_0, where the validity of elasticity theory is obviously questionable. Therefore, this minimum has no physical meaning within the framework of the elastic model.

3.5.2
Predicted Activation Parameters

Knowing the expression of the total energy, it is straightforward to determine the activation parameters E_a and R_c as a function of the stress or the deformation. R_c corresponds to the maximum energy, which is obtained when $\partial E(R)/\partial R = 0$ or

$$\frac{\mu b^2(2-\nu)}{8(1-\nu)}\left(\ln\left(\frac{8m\alpha R_c}{b}\right)-1\right) + (\gamma_f - 2\mu b(1+\nu)s\varepsilon)\pi R_c \pm b_e\cos(\theta)\gamma_s = 0$$

(3.8)

in the case of an applied deformation ε. There is no analytical solution, and R_c has to be determined numerically. Once $R_c(\varepsilon)$ is known, $E_a(\varepsilon) = E(R_c, \varepsilon)$ is easily computed.

Figure 3.6 shows the variation of $R_c(\varepsilon)$ and $E_a(\varepsilon)$ as a function of ε using the same parameters as in Figure 3.5. In the regime of small deformation, both the predicted activation energy and the critical radius are large, suggesting that a thermally activated dislocation nucleation is highly unlikely. An increase of the applied stress leads to a sharp decrease of both quantities, approximately according to a $1/\varepsilon$ relation. It is difficult to set a defined boundary, but one can reasonably consider that the onset of plasticity by half-loop dislocation nucleation would occur when E_a becomes lower than about 2 eV. In fact, a rough estimation of the time required to activate one event at room temperature for such an activation energy is on the order of the duration of a usual deformation experiment. For high applied stresses, both activation energies and critical radius are predicted to decrease. Finally, when the strain (or equivalently the stress) is larger than the athermal threshold, defined in Section 1.4.2, the activation energy vanishes.

3.5.3
What is Missing?

In order to use the elastic model, one has to determine two parameters: m that is a geometrical factor and α that is linked to the dislocation core radius. In the original
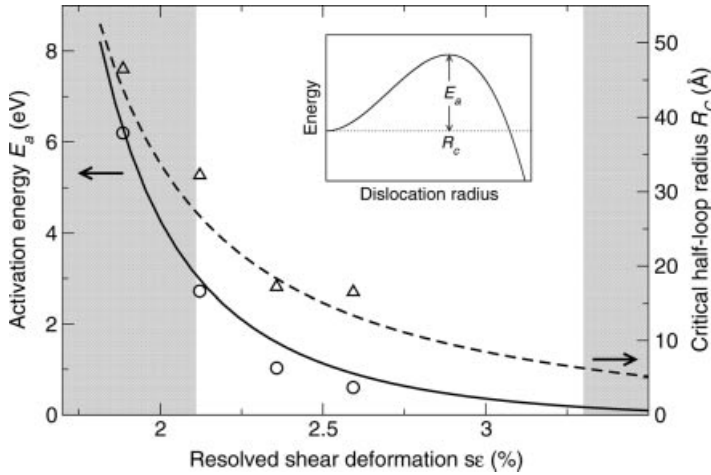
Figure 3.6 Variation of the activation energy E_a (left scale) and critical radius R_c (right scale) as a function of the resolved shear strain $s\varepsilon$ for similar parameters than in Figure 3.5. Open symbols are data obtained from atomistic calculations. For small deformations (left gray area), a thermal activation of the nucleation mechanism is unlikely. For large deformations (right gray area), the validity of the elastic model is questionable. Inset recalls the definition of E_a and R_c, as in Figure 3.3.

formulation of Beltz and Freund, m was determined for a specific geometry and it varies from 0.5 to 0.6 for a Poisson ratio ranging from 0 to 0.5. However, the extent of variation in a general case is not known. Besides, it is not possible to determine accurately α, which is often set to values between 2 and 4 in elasticity studies. Unknowns m and α are not independent in (3.3), meaning that only the product $m\alpha$ has to be determined. Such a feat could be achieved using numerical simulations at the atomistic level, as will be shown in the following section.

Moreover, this elastic model is built on several assumptions. For instance, in the Beltz–Freund derivation of (3.3), the half-loop dislocation is assumed to be perfectly circular. However, in the general case, a full dislocation loop is likely to adopt an elliptical shape, since edge and screw dislocation segments have different energies and mobilities. An elliptical half-loop dislocation could be taken into account in the elastic model, with the transformation $R^2 \rightarrow eR^2$ in (3.5) and (3.7), and $R \rightarrow eR$ in (3.6). The parameter e defines the ellipticity of the loop.

Other assumptions concern the determination of the resolved shear stress on the dislocation from the applied deformation, or conversely. There are two issues here. One is related to the use of linear isotropic elasticity theory, which could not be well suited for strongly anisotropic materials, or for large applied deformations. The other is the inhomogeneous character of the stress depending on the system geometry. In fact, the presence of an initial step on the surface obviously changes the stress distribution. As shown by several authors, there is a stress increase in the vicinity of the step [24, 25]. This is expected to favor dislocation formation and is not taken into account in the elastic model, which assumes an homogeneous stress distribution.

Finally, one has to keep in mind that the validity of the elastic model becomes questionable when R_c is on the same order than the unknown dislocation core radius r_0. Therefore, it is doubtful that it could be used for determining σ_c, the critical stress for which the energy barrier is vanishing. In this particular case, it appears necessary to use atomistic modeling. The latter could also be necessary for investigating systems with a large lattice friction. Indeed, the modification of the atomic environment at the surface is expected to change this lattice friction, which may be locally higher than that in the bulk. Therefore, an additional energy barrier for the very first steps of dislocation nucleation, due to the surface (or the step), could be the critical factor. Additional effects like surface or step reconstructions are also expected to influence the nucleation process. These atomistic effects are clearly not described in the elastic model.

3.5.4
Peierls–Nabarro Approaches

It is possible to make more accurate investigations of the dislocation nucleation process by incorporating selected information at the atomic scale. The well-known Peierls–Nabarro approach allows solving some of the previous issues, however at the expense of an increased complexity. Hence, extensions of the original 1D Peierls–Nabarro model [26, 27] have been developed for dealing with similar 2D and 3D problems [28–30]. The dislocation nucleation from a surface has been investigated by Li and Xu using a general variational boundary integral formulation of Peierls–Nabarro model [31]. This framework allows to deal with complex system, but requires the use of numerical simulations like finite element calculations. Li and Xu showed that an increase of the step height leads to a large reduction in the activation energy and studied the influence of slip plane and step inclinations.

Compared to the above elastic model, the stress inhomogeneity is taken into account in these calculations. Also, there are no limitations regarding the shape of the dislocation loop. Partial information on the dislocation core is included in the calculations through empirical models or from generalized stacking fault surfaces determined with atomistic simulations. Nevertheless, it is of interest to note that the dislocation core is still approximately described within these approaches, and that the influence on the nucleation process of atomistic details of the surface and step cannot be dealt with.

3.6
Atomistic Modeling

In order to remove the limitations reported in the previous section and to determine the input parameters in the elastic model, theoretical investigations can be made by using atomistic simulation methods. Within this framework, the description of the dislocation nucleation process is done at the atomistic level, which allows access to the very beginning of a half-loop dislocation formation. Generally, one can also expect

a better accuracy than with elasticity theory. Unfortunately, it is not all rosy. The first downside of these methods is the usually large computational effort, which results in strong limitations in the size of the considered system and in the timescale for dynamic simulations. This aspect is especially important for first-principles calculations, for which simulations typically include only few hundreds of atoms, with durations on the order of picoseconds. Other methods such as classical molecular dynamics allow to deal with much bigger systems with larger timescale, although the characteristic duration of such a simulation is typically in the nanosecond range. Classical simulations also generally imply an undefined loss of accuracy compared to first-principles calculations.

The second downside of atomistic simulations is that the general nature of the elastic treatment is lost. In fact, it is more difficult to determine a general behavior since the investigated process can depend on the atomistic details of the input system, such as the structure of the surface or a step. More simulations are then required to study the possible configurations.

3.6.1
Examples of Simulations

Most of the few atomistic investigations of dislocation nucleation from surfaces are recent and are focused on simple materials. The aim appears to be a full understanding of the process rather than to numerically reproduce experiments made with real and complex systems. The nucleation of a half-loop dislocation in a ductile simple fcc metal like aluminum has been studied by the authors. Classical molecular dynamics simulations at RT of a stressed Al(100) slab showed the formation of a half-loop partial dislocation from steps initially built on the surface (Figure 3.7) [32]. The nucleation started at an imposed tensile strain of about 6% (with an orientation perpendicular to the surface step), the dislocation gliding in the (111) plane in the continuity of the surface step. Analyses of the dislocation revealed a 90° orientation as expected, since it corresponds to the largest Schmid factor. An equivalent result was obtained in copper by Zhu *et al.* [33], as they investigated the formation of a half-loop partial dislocation from the flat (001) surfaces of a ⟨100⟩ square section nanowire under compressive stress, and for Al and Ni in the case of dislocation nucleation from surfaces at crack tips [34].

Covalent systems have also been considered, aiming at a better understanding of the mechanisms relaxing the high stresses that may occur in the thin layers of semiconductor devices [35]. For instance, Izumi and Yip have studied the formation of a dislocation in silicon from a sharp corner, which is equivalent to a high and straight step [36]. The nucleated dislocation exhibits a half-hexagonal shape, which is characteristic of deep Peierls valleys as expected in covalent materials, and glides in the dense ⟨111⟩ planes. Similar results were obtained for smaller steps by the present authors (Figure 3.8). We have also shown that depending on the range of applied strain and temperature, both partial and perfect dislocations could be nucleated [37, 38], a situation equivalent to what is observed in bulk silicon [8, 39].
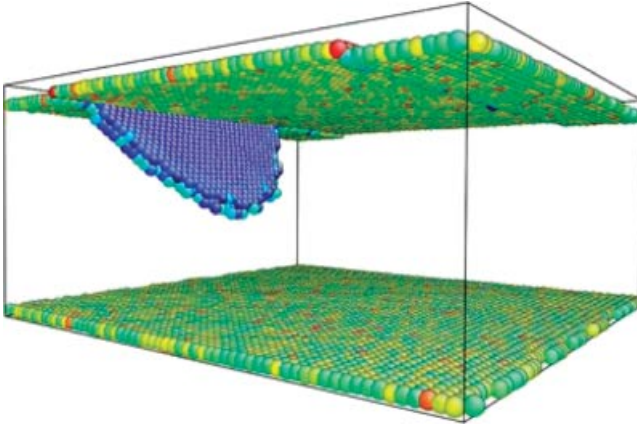
Figure 3.7 Snapshot of a molecular dynamics run at RT showing the formation of a half-loop partial dislocation in a Al(100) slab, leaving a stacking fault connecting with a step on the surface. Only atoms in a nonbulk environment are represented to ease the visualization. With the chosen color code, the dislocation core and stacking fault are represented by blue atoms, whereas atoms forming the surface step are red.

3.6.2
Determination of Activation Parameters

The usual and most appealing simulation framework for investigating thermally activated atomistic processes is molecular dynamics [40, 41], since it allows mimicking the dynamical behavior of the system within various conditions. However, due to computing limitations, the timescale of simulations is severely restricted, which
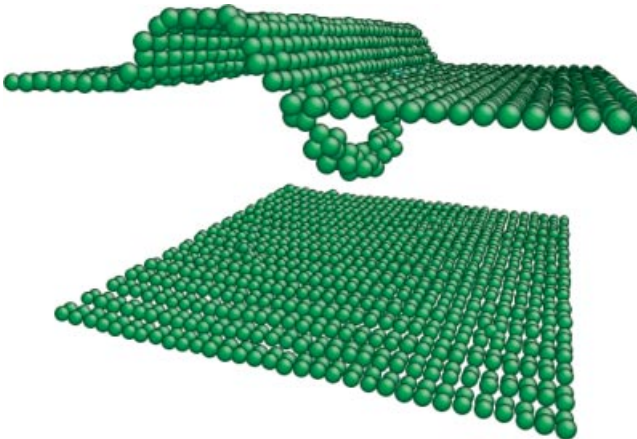

Figure 3.8 Snapshot of a molecular dynamics run at 600 K showing the formation of a half-loop dislocation in a Si(100) slab, starting from a (111) edge. Only atoms in a nonbulk environment are represented to make the visualization easier.

prevents an efficient exploration of the onset of plasticity. In fact, the latter occurs, thanks to a single event, the first nucleated dislocation being usually followed by many others. In an experiment, the probability to observe this initial process is not negligible at moderate stress due to macroscopic timescale. With molecular dynamics, very high stresses, close to the athermal threshold, have to be reached for making the activation possible in the simulations. As a consequence, only a very small stress range could be investigated, and this approach appears to be not suited for a quantitative determination of the activation energy.

Alternative methods to investigate activated processes with high-energy barriers (i.e., rare events) are available. Among the many different flavors of transition-state determination techniques, a chain-like method such as nudged elastic band (NEB) [42] is a favorite nowadays since it is fast, easy to use, and implemented in several computational packages. In an NEB calculation, a set of image configurations allowing to transform a given system from an initial to a final state are first built, and the consecutive images are then linked by springs in configurational space. The relaxation of these images leads to the minimum energy path (MEP), from which the activation energy can be easily deduced. Note that the use of such a method for dislocation nucleation is somewhat tricky [43, 44].

Figure 3.6 shows the critical radii and activation energies determined by NEB calculations for four different applied strains, in the case of an (001) aluminum surface including a one-layer width step. These values have been used for fitting the elastic model described above, considering that the dislocation half-loop may be elliptical. The best fit is reached for $m\alpha = 1$ and an ellipticity factor $e = 1.05$, both reasonable numbers. In fact, using $m \sim 0.5$, a value close to the one given in the original paper from Beltz and Freund, the core radius factor α is found to be about 2. Besides, e is close to 1, justifying the use of the circular half-loop approximation in this specific case. This point is confirmed by the analysis of the shape of the half-loop dislocation, which can be accessed from NEB calculations. Finally, this result indicates that the developed elastic model is sound and captures most of the physical aspects underlying the nucleation of half-loop dislocation from surfaces, at least for fcc metals.

It is worth to mention two shortcomings of the approach. First, although a constant applied stress is assumed in the elastic model, atomistic simulations have been performed with a constant applied strain. In the latter, the resolved shear stress is expected to decrease when a dislocation is formed and propagates through the system, a property that is not included in the elastic model. Second, an NEB calculation is intrinsically static, that is, it only allows computing the internal energy barrier and not the free energy barrier. Vibrational contributions, which are known to be important for many dynamical systems, and inertia effects are not accessible with the NEB method, unlike molecular dynamics. It is difficult to estimate the importance of both issues on the activation energy and the critical radius curves.

3.6.3
Comparison with Experiments

Ideally, the next step would be a thorough comparison of predictions given by the theoretical approaches with available experimental data. Unfortunately, such a feat is

difficult to achieve. We have already mentioned that the true onset of plasticity is difficult to measure in nanoscaled systems. Furthermore, the modeling corresponds to an ideal material that can be relatively far from the real material. For instance, it is well known that most of the mechanical tests of nanopillars have been performed with samples prepared using a focused ion beam technique, which tends to leave a nonnegligible concentration of Ga atoms in the surface.

Nevertheless, theoretical approaches are expected to provide the correct orders of magnitude when compared to experiments. Navarro *et al.* have recently examined the onset of plasticity from gold surfaces with nanoindentation [45]. The measured shear stress are 2.1 and 1.6 GPa for flat and stepped surfaces, respectively. In the case of Al investigated here, the computed values for the elastic limit correspond to yield strengths of few GPa, thus in the same range.

Generally, it seems that theoretical data are overestimated compared to experiments, typically by a factor of 2 or 3. The most likely explanation for this discrepancy is the difference in space and timescales between numerical simulations and experiments. In fact, due to computer limitations, molecular dynamics calculations are usually limited to tens of nanoseconds. Accordingly, the strain/strain rates used in the numerical simulations are unrealistically high [33]. Since the nucleation of the initial dislocation is a stochastic event, the associated onset of plasticity is most likely to occur during an experiment time on the order of a second. As a result, higher stress is required in simulations for initiating plasticity. This issue is known for the investigation of dislocation mobility in bulk materials [46, 47] and has been recently examined for the nucleation of dislocations in nanomaterials [33, 43]. Another possible discrepancy origin is the difference in dimensions between simulations and experiments. For instance, periodic boundary conditions are mostly used for modeling infinitely long nanowires from a small system. The number of possible nucleation sites is, therefore, much smaller than that in a real sample, which makes the dislocation nucleation less likely in simulations. These aspects should be kept in mind when comparing modeling with experiments.

3.6.4
Influence of Surface Structure, Orientation, and Chemistry

In the elastic model described in the previous section, we have considered the general case of a surface, with a step of arbitrary height or without. Nevertheless, a step is generally used in atomistic studies, for it has been shown not only to decrease the amount of strain required for dislocation nucleation but also to localize the nucleation event. Now, since the elastic model has been fitted by considering stepped surfaces, the stress modification due to the step is taken into account, although it is not explicitly included in the model. Test simulations, performed for flat surfaces, suggest that this effect could amount to several tens of electron volts for large applied strains. Recently, Li and Xu have investigated the effect of step height and angle relative to the surface using a Peierls–Nabarro framework [31]. A significant reduction of the required stress is obtained when the step height increases, this effect being stronger for low angles. This result was recently confirmed by atomistic

simulations in metallic systems [43]. These investigations also revealed a nonmo-
notonous behavior between mono- and multilayer steps, which seems to be linked
with the atomic structure of the step. In a covalent material like silicon with a strong
directional bonding, such an effect is expected to be even more important. In these
materials, dislocation cores are usually complex [39] and several step geometries are
possible. Godet *et al.* have shown that the initial formation of the core would depend
on the step geometry [48].

   Other aspects such as the influence of kinks on the steps and of the surface
chemistry have not been extensively studied. Atomistic simulations aiming at
the formation of dislocations from steps with kinks suggested that kinks are not
favorable nucleation sites [32]. This point is supported by experimental evidences that
dislocation nucleation is easier from straight than irregular steps (B. Pichaud, private
communication). The structure of the surface has also been shown to have a
paramount importance for the nucleation process. In fact, first-principles simula-
tions of silicon surfaces under stress [49] revealed that while dislocation formation
succeeded from bare reconstructed surfaces, the nucleation is hindered when the
surface is passivated with hydrogen (Figure 3.9). This result obviously calls for
additional investigations.

   Finally, there have been very few investigations of the influence of the surface
orientation regarding the dislocation formation process. Different orientations
would mean the selection of different slip planes, as well as different step geometries.
Although the atomic structure is not taken into account in their analysis, Li and Xu
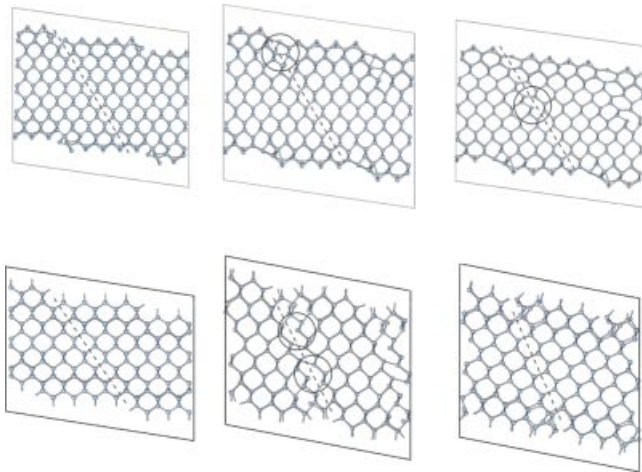have shown that when the angle between the surface and the slip plane is smaller,

Figure 3.9 Successive steps (from left to right) of the first-principles relaxation of a stressed silicon slab. At the top, a single dislocation is nucleated at the step edge and propagates toward the opposite surface. At the bottom, the presence of hydrogen atoms passivating the surface prevents the dislocation formation at the surface, which occurs by homogeneous nucleation into the slab.
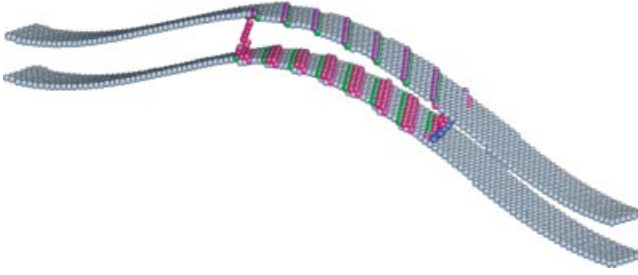
Figure 3.10 Snapshot of a thin buckled Al slab after the nucleation and propagation of several partial dislocations, resulting from the modeling of a delamination process. Only atoms in a nonbulk environment are shown for clarity. Courtesy of J. Durinck *et al.* [51]

dislocation nucleation becomes easier. In the different context of brittle-to-ductile transition, an atomistic study of dislocation emission from crack tip also pointed to a significant effect of the surface orientation [50].

3.7
Extension to Different Geometries

The elastic and atomistic modeling of the onset of plasticity described in the previous sections deals with flat surfaces, eventually containing steps, under the action of a unixial stress (strain), which is rather typical of epitaxial thin films. However, there are other configurations for which the dislocation nucleation from surfaces is expected to be the main plastic mechanism. For instance, molecular dynamics studies of the buckling of metallic thin films revealed the nucleation of many dislocations from the surface (Figure 3.10). Other cases include the nucleation of dislocation from crack tip [52].

The process of dislocation nucleation from surfaces has recently regained attention with the development of nanowire/nanopillar deformation tests [11, 53–57]. Most of the investigations performed with atomistic simulations focused on cylindrical nanowires with diameters usually lower than 10 nm. For fcc metals, a general result of these simulations is the nucleation of dislocations from the surface [58–60]. For such small diameters, the curvature of the surface wire is large and is clearly expected to play a significant role in the process of nucleation. This aspect is not included in the model described in the previous sections, and to our knowledge no attempts have been made to develop an appropriate framework. Nevertheless, experimentally investigated metallic nanopillars have much larger diameters, generally greater than 200 nm. In this case, the surface curvature is small and large flat terraces are likely to exist. The model of surface nucleation should therefore be appropriate.

Atomistic simulations have also been performed for small nanowires made of covalent materials, with a focus on the size effect in the brittle-to-ductile transition [61, 62]. Conversely to metals, very thin covalent nanowires can be synthesized.

Although almost spherical nanowires have been studied, reconstructed facets should be predominant for low-diameter nanowires. The influence of the nanowire section shape then becomes another factor to consider [63]. Note that in the case of a nonrealistic square Cu nanowire, the onset of plasticity has been predicted to occur from dislocation nucleation at the edge rather than at the surface [33].

3.8
Discussion

In this chapter, we have investigated the onset of plasticity in single-crystalline materials having one or several nanometric dimensions, in the framework of elasticity theory and atomistic simulations. The elastic modeling of the nucleation of a dislocation from a surface allows a qualitative description of the process. This model requires to be fitted on atomistic simulations, and one may wonder whether its use is judicious if these simulations have to be performed for each new system. However, it has been shown that only one parameter has to be fitted, and that the resulting value was close to what could be expected. Accordingly, one can tentatively assume that the proposed elastic model could be used for investigating the dislocation nucleation process in other metals like Au, Ag, Pb, or Ni, simply by using the correct physical data and the same fitted parameter. Conversely, for other families of materials such as bcc metals or covalent systems, further atomistic investigations are certainly required.

We have discussed in the preceding sections several issues that tend to make harder the numerical determination of quantities such as the critical stress corresponding to the onset of plasticity in experiments. Yet, the effect of the large differences in timescale and space scale between experiments and simulations has been examined by several authors, and ways to solve the problems have been proposed. Therefore, it should be possible to use the model described here to compute critical stresses for different systems, apply the proposed corrections, and compare with available experiments. To our knowledge, such a systematic comparison remains to be made. Besides, yield stress estimations proposed in experimental papers are usually derived from crude assumptions.

For the specific case of nanowires and nanopillars, the effect of size should be examined. In particular, for the smaller ones, it would be necessary to take into account the surface curvature. This is especially important for nanowires with midrange diameters, too large to be dealt with atomistic simulations, but for which these effects could be important.

Finally, in experiments, the onset of plasticity due to the nucleation of an initial dislocation is often followed by the formation and propagation of other dislocations in adjacent planes. A similar avalanche mechanism, spanning a very short time, is seen in atomistic simulations. The formation of these successive dislocations seems to be easier, thanks to a dynamical and geometrical effect. Nevertheless, a full understanding of this process is still lacking, which would certainly help for a better comparison between experiments and simulations.

References

1 Zhu, T. and Li, J. (2010) Ultra-strength materials. *Prog. Mater. Sci.*, **55**, 710.

2 Uchic, M.D., Dinmiduk, D.M., Florando, J.N., and Nix, W.D. (2004) Sample dimensions influence strength and crystal plasticity. *Science,* **305**, 986.

3 Kizuka, T., Takatani, Y., Asaka, K., and Yoshizaki, R. (2005) Measurements of the atomistic mechanics of single crystalline silicon wires of nanometer width. *Phys. Rev. B*, **72**, 035333.

4 Michler, J., Wasmer, K., Meier, S., Östlund, F., and Leifer, K. (2007) Plastic deformation of gallium arsenide micropillars under uniaxial compression at room temperature. *Appl. Phys. Lett.*, **90**, 043123.

5 Gerberich, W.W., Michler, J., Mook, W.M., Ghisleni, R., Östlund, F., Stauffer, D.D., and Ballarini, R. (2009) Scale effects for strength, ductility, and toughness in "brittle" materials. *J. Mater. Res.*, **24** (3), 898.

6 Frank., F.G. (1950) The origin of dislocations, in *Symposium on Plastic Deformation of Crystalline Solids*, Carnegie Institute of Technology, Pittsburg, CA, p. 89.

7 Matthews, J.W., Blakeslee, A.E., and Mader, S. (1976) Use of misfit strain to remove dislocations from epitaxial thin films. *Thin Solid Films*, **33**, 253.

8 Hirth, J.P. and Lothe, J. (1982) *Theory of Dislocations*, John Wiley & Sons, Inc., New York.

9 Nabarro, F.R.N. (1967) *Theory of Crystal Dislocations*, Oxford University Press, London.

10 Maaß, R., Van Petegem, S., Zimmermann, J., Borca, C.N., and Van Swygenhoven, H. (2008) On the initial microstructure of metallic micropillars. *Scr. Mater.*, **59**, 471.

11 Gerberich, W.W., Michler, J., Mook, W.M., Ghisleni, R., Östlund, F., Stauffer, D.D., and Ballarini, R. (2009) Scale effects for strength, ductility, and toughness in "brittle" materials. *J. Mater. Res.*, **24**, 898.

12 Frank, F.C. and Read, W.T., Jr. (1950) Multiplication processes for slow moving dislocations. *Phys. Rev.*, **79**, 722.

13 Weinberger, C.R. and Cai, W. (2008) Surface-controlled dislocation multiplication in metal micropillars. *Proc. Natl. Acad. Sci. USA*, **105** (38), 14304.

14 Han, X., Zheng, K., Zhang, Y., Zhang, X., Zhang, Z., and Wang, Z.L. (2007) Low-temperature *in situ* large-strain plasticity of silicon nanowires. *Adv. Mater.*, **19** (16), 2112.

15 Scandian, C., Azzouzi, H., Maloufi, N., Michot, G., and George, A. (1999) Dislocation nucleation and multiplication at crack tips in silicon. *Phys. Status Solidi A*, **171** (1), 67.

16 Pichaud, B., Burle, N., Texier, M., Alfonso, C., Gailhanou, M., Thibault-Pénisson, J., Fontaine, C., and Vdovin, V.I. (2009) Dislocation nucleation in heteroepitaxial semiconducting films. *Phys. Status Solidi C*, **6** (8), 1827.

17 Greer, J.R. and Nix, W.D. (2006) Nanoscale gold pillars strengthened through dislocation starvation. *Phys. Rev. B*, **73**, 245410.

18 Phillips, R. (2001) *Crystals, Defects and Microstructures: Modelling across Scales*, Cambridge University Press, Cambridge.

19 Caillard, D. and Martin, J.L. (2003) *Thermally Activated Mechanisms in Crystal*

Plasticity, Pergamon Materials Series, Pergamon.

20 Vineyard, G.H. (1957) Frequency factors and isotope effects in solid state rate processes. *J. Phys. Chem. Solids*, **3**, 121.

21 Kamat, S.V. and Hirth, J.P. (1990) Dislocation injection in strained multilayer structures. *J. Appl. Phys.*, **67** (11), 6844.

22 Zou, J. and Cockayne, D.J.H. (1996) Nucleation of semicircular misfit dislocation loops from the epitaxial surface of strained-layer heterostructures. *J. Appl. Phys.*, **79** (10), 7632.

23 Beltz, G.E. and Freund, L.B. (1993) On the nucleation of dislocations at a crystal surface. *Phys. Status Solidi B*, **180**, 303.

24 Smith, E. (1968) The stress concentration at a step on the surface of a brittle crystalline solid. *Int. J. Eng. Sci.*, **6**, 9.

25 Brochard, S., Beauchamp, P., and Grilhé, J. (2000) Stress concentration near a surface step and shear localization. *Phys. Rev. B*, **61** (13), 8707.

26 Lu, G. (2005) The Peierls–Nabarro model of dislocations: a venerable theory and its current development, in *Handbook of Materials Modeling. Volume I: Methods and Models*, vol. 2.20 (ed. S. Yip), Springer, pp. 1.

27 Schoeck, G. (2005) The Peierls model: progress and limitations. *Mater. Sci. Eng. A*, **400–4001**, 7.

28 Rice, J.R. and Beltz, G.E. (1994) The activation energy for dislocation nucleation at a crack. *J. Mech. Phys. Solids*, **42** (2), 333.

29 Lu, G., Bulatov, V.V., and Kioussis, N. (2003) A nonplanar Peierls–Nabarro model and its application to dislocation cross-slip. *Philos. Mag.*, **83** (31–34), 3539.

30 Denoual, C. (2007) Modeling dislocation by coupling Peierls–Nabarro and element-free Galerkin methods. *Comput. Methods Appl. Mech. Eng.*, **196**, 1915.

31 Li, C. and Xu, G. (2006) Critical conditions for dislocation nucleation at surface steps. *Philos. Mag.*, **86** (20), 2957.

32 Hirel, P., Brochard, S., Pizzagalli, L., and Beauchamp, P. (2007) Effects of temperature and surface step on the incipient plasticity in strained aluminium

studied by atomistic simulations. *Scr. Mater.*, **57**, 1141.

33 Zhu, T., Li, J., Samanta, A., Leach, A., and Gall, K. (2008) Temperature and strain-rate dependence of surface dislocation nucleation. *Phys. Rev. Lett.*, **100**, 025502.

34 Warner, D.H. and Curtin, W.A. (2009) Origins and implications of temperature-dependent activation energy barriers for dislocation nucleation in face-centered cubic metals. *Acta Mater.*, **57**, 4267.

35 Izumi, S., Miyake, T., Sakai, S., and Ohta, H. (2005) Application of three-dimensional dislocation dynamics simulation to the STI semiconductor structure. *Mater. Sci. Eng. A*, **395**, 62.

36 Izumi, S. and Yip, S. (2008) Dislocation nucleation from a sharp corner in silicon. *J. Appl. Phys.*, **104**, 033513.

37 Godet, J., Hirel, P., Brochard, S., and Pizzagalli, L. (2009) Evidence of two plastic regimes controlled by dislocation nucleation in silicon nanostructures. *J. Appl. Phys.*, **105**, 026104.

38 Godet, J., Hirel, P., Brochard, S., and Pizzagalli, L. (2009) Dislocation nucleation from surface step in silicon: the glide set versus the shuffle set. *Phys. Status Solidi A*, **206** (8), 1885.

39 Rabier, J., Pizzagalli, L., and Demenet, J.-L. (2010) Dislocations in silicon at high stress, in *Dislocation in Solids*, vol. 16 (eds L. Kubin and J.P. Hirth), Elsevier, Chapter 93, pp. 47.

40 Allen, M.P. and Tildesley, D.J. (1989) *Computer Simulation of Liquids*, Clarendon Press, Oxford.

41 Thijssen, J.M. (2000) *Computational Physics*, Cambridge University Press, Cambridge.

42 Jónsson, H., Mills, G., and Jacobsen, K.W. (1998) Nudged elastic band method for finding minimum energy paths of transitions, in *Classical and Quantum Dynamics in Condensed Phase Simulations* (eds B.J. Berne, G. Ciccotti, and D.F. Coker), World Scientific, Chapter 16, pp. 385.

43 Brochard, S., Hirel, P., Godet, J., and Pizzagalli, L. (2010) Elastic limit for surface step dislocation nucleation in face-centered cubic metals: temperature

and step height dependence. *Acta Mater.*, **58**, 4182.

44 Zhu, T., Li, J., Samanta, A., Kim, H.G., and Suresh, S. (2007) Interfacial plasticity governs strain rate sensitivity and ductility in nanostructured metals. *Proc. Nat. Acad. Sci. USA*, **104** (9), 3031.

45 Navarro, V., Rodrìguez de la Fuente, O., Mascaraque, A., and Rojo, J.M. (2008) Uncommon dislocation processes at the incipient plasticity of stepped gold surfaces. *Phys. Rev. Lett.*, **100**, 105504.

46 Domain, C. and Monnet, G. (2005) Simulation of screw dislocation motion in iron by molecular dynamics simulations. *Phys. Rev. Lett.*, **95**, 215506.

47 Rodney, D. (2007) Activation enthalpy for kink-pair nucleation on dislocations: comparison between static and dynamic atomic-scale simulations. *Phys. Rev. B*, **76**, 144108.

48 Godet, J., Pizzagalli, L., Brochard, S., and Beauchamp, P. (2004) Theoretical study of dislocation nucleation from simple surface defects in semiconductors. *Phys. Rev. B*, **70**, 54109.

49 Godet, J., Brochard, S., Pizzagalli, L., Beauchamp, P., and Soler, J.M. (2006) Dislocation formation from a surface step in semiconductors: an *ab initio* study. *Phys. Rev. B*, **73**, 092105.

50 Hess, B., Thijsse, B.J., and Van der Giessen, E. (2005) Molecular dynamics study of dislocation nucleation from a crack tip. *Phys. Rev. B*, **71**, 054111.

51 Durinck, J., Coupeau, C., Colin, J., and Grilhé, J. (2008) Molecular dynamics simulations of buckling-induced plasticity. *Appl. Phys. Lett.*, **93**, 221904.

52 Zhu, T., Li, J., and Yip, S. (2004) Atomistic study of dislocation loop emission from a crack tip. *Phys. Rev. Lett.*, **93** (2), 025503.

53 Nix, W.D., Greer, J.R., Feng, G., and Lilleodden, E.T. (2007) Deformation at the nanometer and micrometer length scales: Effects of strain gradients and dislocation starvation. *Thin Solid Films*, **515**, 3152.

54 Volkert, C.A. and Lilleodden, E.T. (2006) Size effects in the deformation of sub-micron Au columns. *Philos. Mag.*, **86**, 5567.

55 Mook, W.M., Lund, M.S., Leighton, C., and Gerberich, W.W. (2008) Flow stresses and activation volumes for highly deformed nanoposts. *Mater. Sci. Eng. A*, **493**, 12.

56 Ho Oh, S., Legros, M., Kiener, D., and Dehm, G. (2009) In situ observation of dislocation nucleation and escape in a submicrometre aluminium single crystal. *Nat. Mater.*, **8**, 95.

57 Östlund, F., Rzepiejewska-Malyska, K., Leifer, K., Hale, L.M., Tang, Y., Ballarini, R., Gerberich, W.W., and Michler, J. (2009) Nanostructure Fracturing: Brittle-to-Ductile Transition in Uniaxial Compression of Silicon Pillars at Room Temperature. *Adv. Funct. Mater.*, **19**, 2439.

58 Park, H.S., Gall, K., and Zimmerman, J.A. (2006) Deformation of fcc nanowires by twinning and slip. *J. Mech. Phys. Solids*, **54**, 1862.

59 Rabkin, E., Nam, H.-S., and Srolovitz, D.J. (2007) Atomistic simulation of the deformation of gold nanopillars. *Acta Mater.*, **55**, 2085.

60 Deng, C. and Sansoz, F. (2009) Fundamental differences in the plasticity of periodically twinned nanowires in Au, Ag, Al, Cu, Pb and Ni. *Acta Mater.*, **57**, 6090.

61 Kang, K. and Cai, W. (2007) Brittle and ductile fracture of semiconductor nanowires: molecular dynamics simulations. *Philos. Mag.*, **87** (14–15), 2169.

62 Wang, Z., Zu, X., Yang, L., Gao, F., and Weber, W.J. (2007) Atomistic simulations of the size, orientation, and temperature dependence of tensile behavior in GaN nanowires. *Phys. Rev. B*, **76**, 045310.

63 Justo, J.F., Menezes, R.D., and Assali, L.V.C. (2007) Stability and plasticity of silicon nanowires: the role of wire perimeter. *Phys. Rev. B*, **75**, 045303.